separations

MDPI

Article

A Pilot-Scale Treatment of Steel Plant Wastewater by PVDF Hollow Fiber Ultrafiltration Membrane with Low Packing Density

Yangang Zhang [1,2], Zhangfu Yuan [1], He Bai [3], Linfei Zhao [1,*], Liudong He [2] and Chunhong Shi [4]

[1] Collaborative Innovation Center of Steel Technology, University of Science and Technology Beijing, Beijing 100083, China; zhang.yangang@scinorwater.com (Y.Z.); zfyuan2016@ustb.edu.cn (Z.Y.)
[2] Beijing Scinor Water Technology Co., Ltd., Beijing 100083, China; liuhedong@126.com
[3] Beijing Scinor Membrane Technology Co., Ltd., Beijing 100083, China; bai.he@scinormem.com
[4] School of Energy and Environmental Engineering, University of Science and Technology Beijing, Beijing 100083, China; sch.22@163.com
* Correspondence: zhaolinfei2021@163.com

Abstract: The treatment of wastewater from the iron and steel industry is difficult due to its complex and changeable characteristics. This paper introduces the application of polyvinylidene fluoride (PVDF)-pressurized ultrafiltration membrane with low packing density that produced via thermally induced phase separation (TIPS) in wastewater of iron and steel industry, to study the effects of packing density of ultrafiltration membrane modules as well as the membrane performance under different operation conditions, in order to provide guidance for the subsequent development of other ultrafiltration applications in wastewater of iron and steel. The results show a significant positive effect of smaller packing density on the transmembrane pressure difference (TMP) reducing and higher permeability. Under 30 min filtration cycle and 65 L m^{-2} h^{-1} (LMH) operation flux, the permeability can be stabilized to 200 L/(m^2·h)/0.1 MPa, which is two times higher than that of the membrane module with 0.3 m^2/m^3 higher packing density under the same condition. It is obvious that compared with enhanced flux maintenance (EFM), chemically enhanced backwash (CEB) is a more effective cleaning method for iron and steel wastewater, which maintains TMP (30 kPa) without any significant increase under the premise of ensuring the high-flux (65 LMH) operation. The results also suggest reasonable parameters based on the test water quality, which include the filtration cycle and operation flux. The scanning electron microscopy (SEM) analysis and the turbidity of the permeate show that the ultrafiltration membrane has good intercept ability and high anti-pollution performance.

Keywords: steel industry wastewater; ultrafiltration; packing density; membrane cleaning; membrane fouling

check for updates

Citation: Zhang, Y.; Yuan, Z.; Bai, H.; Zhao, L.; He, L.; Shi, C. A Pilot-Scale Treatment of Steel Plant Wastewater by PVDF Hollow Fiber Ultrafiltration Membrane with Low Packing Density. *Separations* **2022**, *9*, 37. https://doi.org/10.3390/separations9020037

Academic Editor: Victoria Samanidou

Received: 29 December 2021
Accepted: 28 January 2022
Published: 30 January 2022

Publisher's Note: MDPI stays neutral with regard to jurisdictional claims in published maps and institutional affiliations.

Copyright: © 2022 by the authors. Licensee MDPI, Basel, Switzerland. This article is an open access article distributed under the terms and conditions of the Creative Commons Attribution (CC BY) license (https://creativecommons.org/licenses/by/4.0/).

1. Introduction

As an important natural resource, water is an indispensable resource for human life and production. It is of great significance for promoting social and economic development and promoting the progress of civilization [1–3]. At present, the world is facing a serious water resource crisis, and a quarter of the world's population is facing water shortages [4]. In order to alleviate the water crisis, the recycling of industrial wastewater has become an important way to solve the water crisis, alleviate the shortage of water resources, and increase the supply of water resources [5–8].

The iron and steel industry is one of the five major water-consuming industries in China. Water consumption in this industry accounts for 20% of the total industrial water consumption, and its wastewater discharge accounts for 11.3% of the total industrial wastewater discharge [9]. In 2020, the annual output of crude steel in China was 1065 billion

tons, with the water demand per ton of steel reaching about 25 T and the fresh water consumption about 2.8 T [10]. However, among the current steel companies, the recycling and treatment of sewage are obviously insufficient, and increasing environmental pollution is traced back to steel companies [11]. To realize the sustainable development of the iron and steel industry, it is necessary to strengthen the recycling of wastewater resources. The iron and steel industry has multiple production processes, and the composition of wastewater is complex [12]. The pollutants are mainly related to suspended solids, chemical oxygen demand (COD_{Cr}), hardness, alkalinity, oils, salts, etc. The complexity, fluctuation, and high conductivity of water make wastewater treatment more difficult [13,14].

Wastewater reuse technologies in the iron and steel industry include physical and chemical water treatment, biochemical water treatment, membrane separation and concentration, and end treatment technologies [15]. Among them, ultrafiltration membrane separation technology is a pressure-driven separation process that can be effectively distributed through micropores distributed on the membrane surface. The interception of bacteria and suspended matter, as well as the COD_{Cr}, total phosphorus, and total nitrogen carried by the suspended matter, is one of the more mature technologies in recent years and is widely used in various fields of water treatment [16,17]. Compared with the traditional advanced treatment technology, the ultrafiltration technology has a simple structure, high degree of automation, convenient operation, small area in the process of iron and steel wastewater treatment, and has great advantages in the removal of suspended solids and microorganisms [18].

For the application of ultrafiltration technology in the wastewater treatment process, many scholars have conducted in-depth studies on this subject, but the practical application of this technology in wastewater treatment of the iron and steel industry and establishing a standard system are not yet perfect [19–22]. The main factors affecting the performance of ultrafiltration are filtration cycle, flux, cleaning mode, and the structure of membrane modules, in which the packing density and the effective length of membrane fiber have the most significant influence on the structural design of modules and become important research directions of each manufacturer.

The fouling rate of modules with low packing density will be greatly reduced since the flow distribution of single fiber changed relatively less, while the flow distribution of modules with high packing density (usually greater than 0.8 m^2/m^3) is uneven, where more driving pressure exists on the feed side. In the meantime, the hydraulic resistance along the fiber cannot be ignored under the condition of high packing density and long fiber length, as the changes in the driving force in the axial direction along the membrane fiber will lead to uneven force and unbalanced fouling [23]. Therefore, with similar fiber lengths, the difference in packing density will become an important influence on filtration performance.

In this study, the effect of ultrafiltration membrane on the treatment of steel wastewater was analyzed, taking the wastewater treatment of a steel enterprise in Shandong, China, as an example, the filtration performance was compared between the membrane module with low packing density and the modules with the same membrane length and other conditions but with higher packing density. Meanwhile, the effects of the filtration cycle, operating flux, and cleaning method on the performance of the membrane module with low packing density were also investigated, to provide a valuable reference for the ultrafiltration treatment process of steel wastewater.

2. Materials and Methods

2.1. Wastewater Effluent

In this study, the wastewater came from an iron and steel enterprise in Shandong, China. The water quality characteristics of the wastewater entering the ultrafiltration system after pretreatment can be observed in Table 1.

Table 1. Main characteristics of the wastewater effluent used in this study.

Item	Unit	Parameter
CODCr	mg/L	19–36
Turbidity	NTU	3–5
SS	mg/L	5–10
Total hardness	mg/L	167–249
Cl^-	mg/L	176–227
Electrical conductivity	$\mu s/cm^2$	1240–1641
Total dissolved solids	mg/L	772–913
Petroleum	mg/L	≤0.04
Anionic surfactant	mg/L	≤0.05
Fe	mg/L	≤0.46
Mn	mg/L	≤0.05
BOD_5	mg/L	≤20
Chromaticity	°	≤30
Total P	mg/L	≤1
NH_{4+}-N	mg/L	≤1
pH		6.8–7.9

2.2. Ultrafiltration Setup

The ultrafiltration process was a membrane separation process with screening as the separation principle and pressure as the driving force. The ultrafiltration membrane can effectively remove suspended solids and various macromolecules in the solution according to its size and trap them outside the membrane. Solvent and small molecules entered the water-producing side through the membrane hole with water. The ultrafiltration membrane module for iron and steel wastewater treatment was the SMT900-P80 module of Beijing Sino Membrane Technology Co., Ltd. (Beijing, China), for the comparison, SMT600-P50, another membrane module of the company, was adopted, which had similar fiber length but higher packing density. The high-precision PVDF hollow fiber ultrafiltration membrane prepared by TIPS was adopted in both modules; it is a homogeneous cavernous structure with characteristics of large throughput, long life, drug resistance, anti-fouling, etc. The dynamic filtration process of the membrane module adopted the form of outside in and inside out, the raw water flowed under pressure outside the membrane, and the intercepted substances were removed with a concentrated solution, so as not to plug the membrane surface. The technical parameters of the two modules are shown in Table 2.

Table 2. Technical parameters of membrane module.

Model	SMT600-P50	SMT900-P80
Material	PVDF	PVDF
Membrane area (m^2)	50	80
Membrane wire inner/outer diameter (mm)	0.7/1.3	0.7/1.3
Packing density (m^2/m^3)	1.27	0.97
Effective fiber length (mm)	1958	2030

2.3. Process Method

Steel wastewater entered the ultrafiltration system after pretreatment, and the system can automatically switch between constant-flux filtration mode and backwash mode.

In the comparison of the performance of membrane modules with different packing densities, SMT900-P80 and SMT600-P50 were operated under the same conditions, with a 30 min filtration cycle and 65 LMH operating flux. Backwashing was automatically performed after each cycle. The backwashing process included 30 s of gas scrubbing, 45 s of combined gas–water backwashing, and 30 s of water backwashing. As TMP increased rapidly when high packing density modules were running, a chemical cleaning in place was performed every 5 days during the operation of SMT600-P50 modules.

During the filtration process, the intercepted impurities accumulated continuously on the membrane surface, resulting in a concentration polarization phenomenon, which reduced the permeability of the membrane. Reasonable operating conditions and cleaning technology can slow down this phenomenon. Therefore, for SMT900-P80, the effects of different operating parameters on the filtration performance were carried out simultaneously.

The effects of three key factors on SMT900-P80 membrane performance—namely, operating flux, filtration cycle, and cleaning mode, were investigated separately in the operation of the ultrafiltration system. All projects were carried out at ambient temperature. The whole process was divided into three stages: The first stage controlled the operating flux of 70 LMH and the filtration cycles of 30 min and 40 min, while the second stage determined the filtration cycle of 30 min and the operating fluxes of 60 LMH, 65 LMH, and 70 LMH, respectively. The third stage determined the filtration cycle to be 30 min with an operating flux of 65 LMH, and the cleaning methods were divided into CEB and EFM. The membrane was soaked with 500 ppm sodium hypochlorite and dosed once a day in CEB, and in EFM, the membrane was soaked with 2000 ppm sodium hypochlorite and 500 ppm sodium hydroxide and dosed once every 10 days. A chemical cleaning in place (CIP) was carried out with 2000 ppm sodium hypochlorite and 2000 ppm sodium oxalate before the operating conditions were switched. Differential pressure transmitters, temperature transmitters, and flow meters were provided on the water production side of the system to check parameters such as differential pressure and water flux.

2.4. Membrane Performance Analysis

The transmembrane pressure difference is the pressure required to drive water through the membrane. A membrane with a smaller pore size requires a larger transmembrane pressure difference. When the water temperature is low, the flux is high, and fouling occurs; an increase in transmembrane pressure difference leads to the solidification of the fouling layer, resulting in irreversible fouling [24]. The transmembrane pressure difference is calculated by Equation (1).

$$\Delta P = P_{\mathrm{f}} - P_{\mathrm{p}} \tag{1}$$

where P_{f} is the inlet water pressure, and P_{p} is the produced water pressure.

The operating effectiveness of the membrane module was characterized by the produced water permeability. The produced water permeability (J) is expressed as the volume of fluid that passed through a unit membrane area per hour when the transmembrane pressure difference is 0.1 MPa. The degree of fouling and the calculation of the permeation ratio of the produced water before and after the membrane cleaning is one of the important methods to judge whether the cleaning plan is effective. The calculation formula of product water permeability is shown in Equation (2). According to Equations (3)–(6), the flux recovery ratio (F_{r}), total fouling ratio (R_{t}), reversible fouling ratio (R_{r}), and irreversible fouling ratio (R_{ir}) were calculated, respectively [25].

$$J = \frac{V}{S \times t \times \Delta \mathrm{P}} \tag{2}$$

where V (L) is the volume of permeable water, S (m^2) is the effective area, and t (h) is the operation time.

$$F_{\mathrm{r}} = \frac{J_1}{J_0} \times 100\% \tag{3}$$

$$R_{\mathrm{t}} = \left(1 - \frac{J_{\mathrm{p}}}{J_0}\right) \times 100\% \tag{4}$$

$$R_{\mathrm{r}} = \frac{J_1 - J_{\mathrm{p}}}{J_0} \times 100\% \tag{5}$$

$$R_{\mathrm{ir}} = \left(1 - \frac{J_1}{J_0}\right) \times 100\% \tag{6}$$

where J_0 is the initial water permeability of the membrane, J_p is the produced water permeability of the contaminated membrane after the operation, and J_1 is the produced water permeability of the contaminated membrane after cleaning.

The retention performance test of the membrane used the turbidity of raw water and produced water as parameters, and the retention ratio (R) was calculated according to Equation (7).

$$R = \left(1 - \frac{S_1}{S_0}\right) \times 100\% \quad (7)$$

where S_0 is the turbidity of the raw water, and S_1 is the turbidity of the produced water.

2.5. Characterization Method

Turbidity was determined with a 6035 turbidimeter from Jenway. The microstructures of the surface and cross-section of the membrane were characterized by FE–SEM (JSM-6701F, Chiba, Japan).

3. Results and Discussion

3.1. Effect of Packing Density on Filtration Performance

One of the characteristics of ultrafiltration membrane fouling is the increase in TMP and the drop of permeability. This paper focused on the changes of the membrane permeability and TMP to evaluate the influence of packing density on the membrane filtration performance by continuous monitoring. As shown in Figure 1, the permeability of the SMT600-P50 membrane module was stable between 50 L/(m^2·h)/0.1 MPa–110 L/(m^2·h)/0.1 MPa during the whole year's operation, and six sets of membrane systems showed similar trends—namely, that the permeability of SMT600-P50 reached 95 L/(m^2·h)/0.1 MPa–105 L/(m^2·h)/0.1 MPa after chemical cleaning but only about 50 LMH at the end of each filtration cycle. By contrast, SMT900-P80 yielded a better result under the same condition, with 30 min filtration cycle and 65 LMH operating flux; permeability was able to be stable at higher than 200 L/(m^2·h)/0.1 MPa for the whole one week cleaning cycle, which was two times of original module, as shown in Figure 2. TMP increase curve showed a similar trend—aside from the average TMP of SMT600-P50 being three times higher than SMT900-P80, the TMP increase in the single filtration period occurred significantly more rapidly.

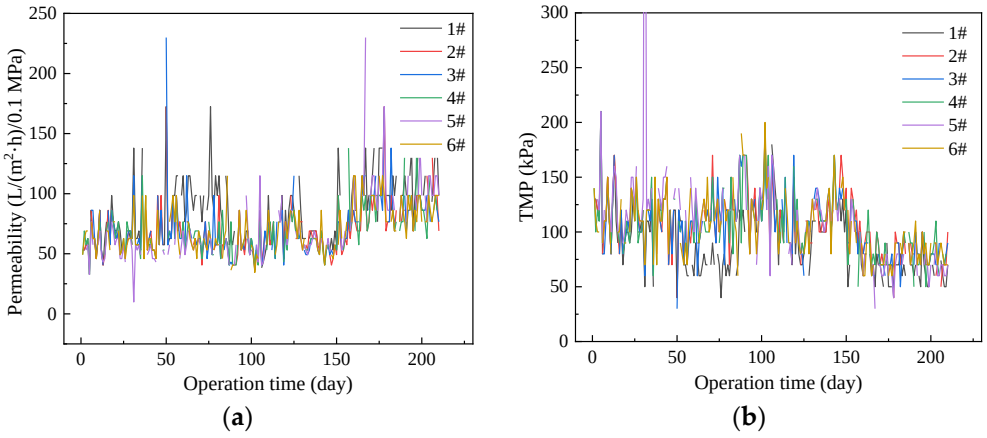


Figure 1. Variation trend of (**a**) permeability and (**b**) TMP of 6 sets of SMT600-P50 membrane systems (1#, 2#, 3#, 4#, 5# and 6#).

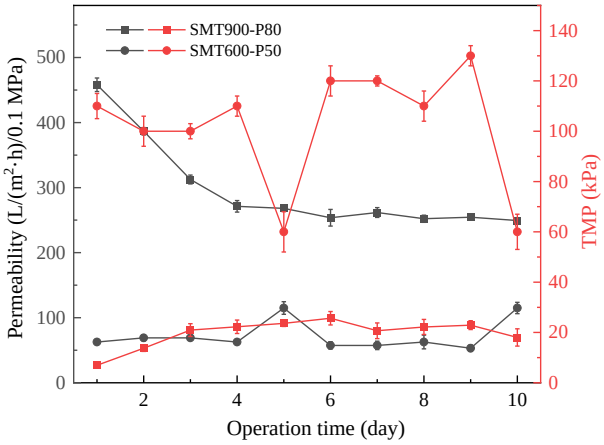


Figure 2. Performance comparison between SMT600-P50 and SMT900-P80.

The differences between the two modules indicated that the packing density plays an important role in the performance of membrane modules. The gap between fibers was the path of water flow, and it also promoted mass transfer through fibers. Favorable hydrodynamic conditions existed inside the low packing density modules, and the central fiber and the top of the fiber maintained high flux, resulting in uniform permeation distribution. Therefore, the SMT900-P80 module with low packing density had superior filtration performance. For the modules with higher packing density, the fluid flow velocity increased due to the space limitation, and the permeation distribution along the fiber length was uneven. At the same time, the fluid flux of the central fiber was significantly lower than that of the external fiber. Therefore, filtration occurred preferentially in the central fiber and the bottom of the fiber, resulting in a decrease in effective filtration area, serious local pollution, and an increase in TMP.

Therefore, this inevitably leads to an increase in cleaning frequency and a reduction in membranes' service life. Another study introduced the concept of net present value (NPV) to evaluate the economics of ultrafiltration systems, and the results showed that an increase in cleaning frequency will bring more chemical agents and energy consumption, which directly leads to the increase in investment costs per ton of water produced [26]. At the same time, too frequent cleaning will inevitably lead to reduced membrane service life, which has an important impact on the NPV value of the whole life cycle. When the service life of membrane modules is less than 3 years, the economic benefits of the whole plant are greatly reduced. In particular, the wastewater quality of the steel industry is more complex, and the possibility of fouling is greater than other applications; thus, in consideration of the overall investment and floor area and other factors, modules with lower packing density should be selected first.

3.2. Effect of Operating Parameters on Filtration Performance of SMT900-P80

In order to further determine the suitable operating conditions of the SMT900-P80 module, the effects of the filtration cycle, operation flux, and cleaning mode on the filtration performance of the SMT900-P80 module were investigated.

The continuous operation process of the ultrafiltration system is an alternating process of filtration and backwashing. The filtration cycle refers to the time interval between the two backwash phases of the ultrafiltration membrane system. Under constant membrane flux operating conditions, extending the filtration cycle can greatly increase the water production ratio of the ultrafiltration membrane system. Figure 3a shows the trend of produced water permeability with operating time under the conditions of an operating flux of 70 LMH and filtration cycle of 30 min and 40 min, respectively. After the 30 min filter cycle was completed, CIP was performed, and it was changed to a 40 min filter cycle. It can be seen that the water permeability decreased significantly when the filtration cycle was 30 min, while the changing trend was more moderate when the filtration cycle was

40 min. After running for the same time, the water permeability at 30 min filtration cycle was always higher than 40 min. At 30 min filtration cycle, the fouling layer was loose and easily removed by backwashing, so the water permeability fluctuated more. However, if the filtration cycle is extended excessively, the membrane module will be in working condition for a long time, and the fouling will be deposited on the membrane surface gradually to block the membrane pores with the membrane filtration process. The filter cake layer will accumulate and become dense, which will lead to regular backwashing to restore the membrane's performance effectively, thus increasing membrane fouling and even causing irreversible fouling. This was confirmed by the trend of the corresponding transmembrane pressure difference in Figure 3b, where the transmembrane pressure difference increased after a period of operation. Therefore, the operation of the ultrafiltration system should choose the appropriate filtration cycle according to the actual situation, and the filtration cycle can be appropriately increased under the premise of ensuring high filtration performance.

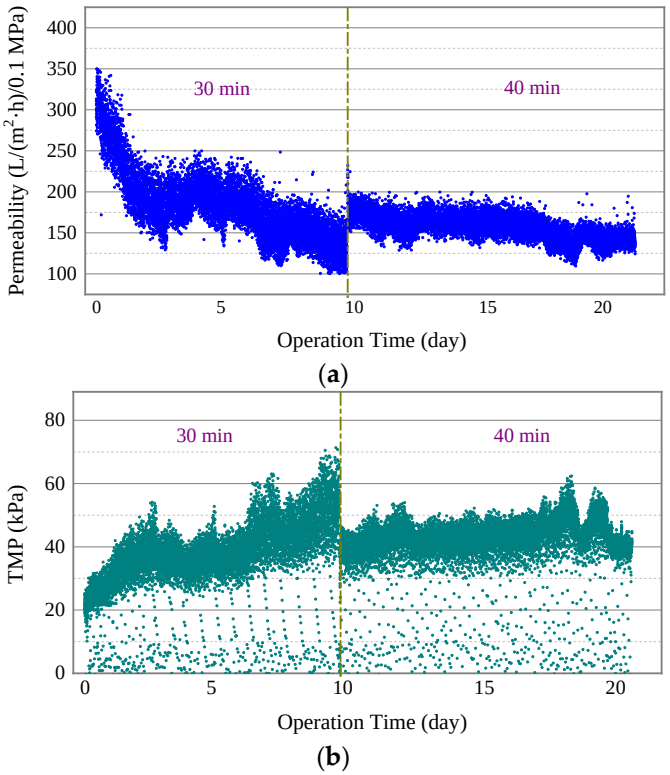


Figure 3. Variation trend of (**a**) permeability and (**b**) TMP under different filtration cycles.

Membrane flux is one of the important factors reflecting membrane performance. High membrane flux means more water can be treated per unit time and unit area. An ultrafiltration system operating with high membrane flux for a long time can treat the same amount of water, which can effectively reduce the frequency of membrane cleaning and replacement and reduce the operation cost. Figure 4a shows the trend of water permeability with operating time for a filtration cycle of 30 min and operating fluxes of 60 LMH, 65 LMH, and 70 LMH, respectively, with CIP before each change of operating flux. Under the three operating flux conditions, the water permeability declined rapidly in the early stage and then stabilized. When using 70 LMH operating flux, the stable zone of water permeability was significantly shorter and fluctuated more than other flux conditions, and the rapid decrease in water permeability appeared again in the middle and late operating curves. At the lower fluxes of 60 LMH and 65 LMH, the membrane fouling was not significant, and the fouling accumulated on the membrane surface to form a looser cake layer, so backwashing could remove the fouling well and prevent the further decrease in water

permeability. A high membrane flux of 70 LMH accelerated the process of membrane fouling and accumulated a large amount of fouling on the membrane surface in a short period of time. As can be seen in Figure 4b, the differential pressure across the membrane for the 70 LMH operating flux increased rapidly, to 50 kPa, resulting in solidification of the contaminant cake layer, which was difficult to remove by backwashing, thus forming irreversible contamination. Meanwhile, it can be seen in Figure 4c,d that the fouling layer on the membrane surface with an operating flux of 70 LMH was thicker and denser than that with 65 LMH. Therefore, to ensure the stability of the system operation, the operating flux should not exceed 65 LMH.

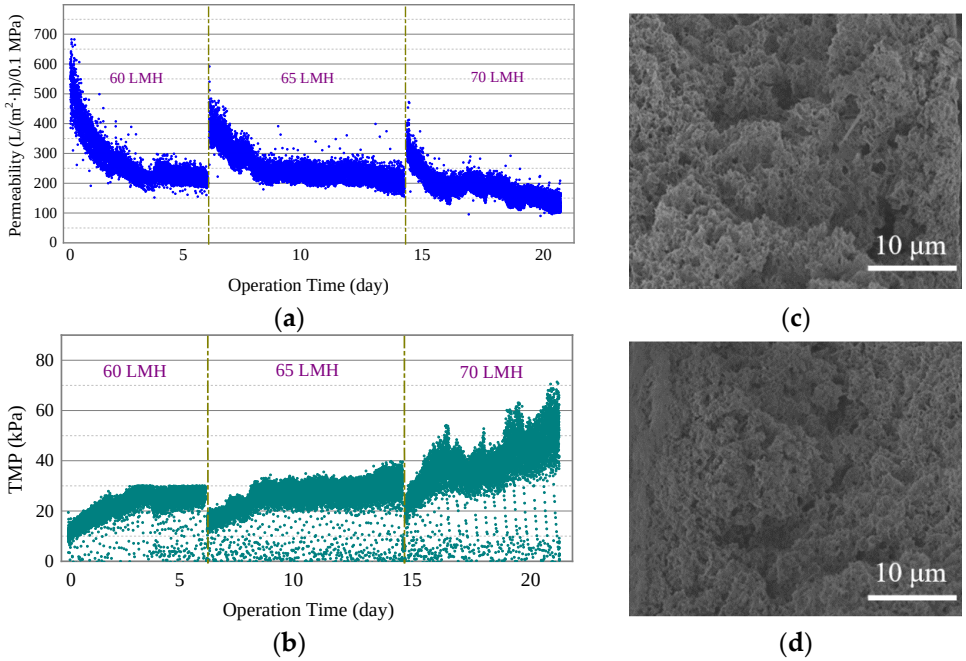


Figure 4. Variation trend of (**a**) permeability and (**b**) TMP under different operating fluxes, and microstructure of membrane outer surface after one-week operation at (**c**) 65 LMH and (**d**) 70 LMH operating fluxes.

A reasonable cleaning method during the operation of the ultrafiltration system can effectively improve the filtration performance of the membrane and reduce the cleaning cost. Under the conditions of a filtration cycle of 30 min and an operating flux of 65 LMH, two cleaning methods, CEB and EFM, were used to clean the membrane. EFM was used on the 10th day of operation, and CIP was performed before switching to the CEB cleaning method. Figure 5a shows the changing trend of water permeability with running time under different cleaning operation conditions; the decreasing trend of water permeability under the CEB method was not obvious, and relatively stable, while the water permeability recovery ratio was higher and more fluctuating due to the addition of chemical reagents in the backwashing process every day. Although the frequency of adding reagents in the EFM method was reduced, the dosage was large, and the trend of decreasing water permeability was obvious, and because of the long operation without chemical reagents, the filter cake layer became thick or even solidified, resulting in the insignificant recovery ratio of water permeability after cleaning; thus, the overall water permeability was lower than the CEB method. Therefore, CEB could ensure the stability of the system and would presumably continue to reduce the amount of chemical use, reducing operating costs. Figure 5b shows that the TMP of the EFM increased sharply and reached 100 kPa by the end of the operation, while the TMP of the CEB started to stabilize after a small increase in the initial stage and was maintained around 30 kPa, which largely reduced the energy consumption.

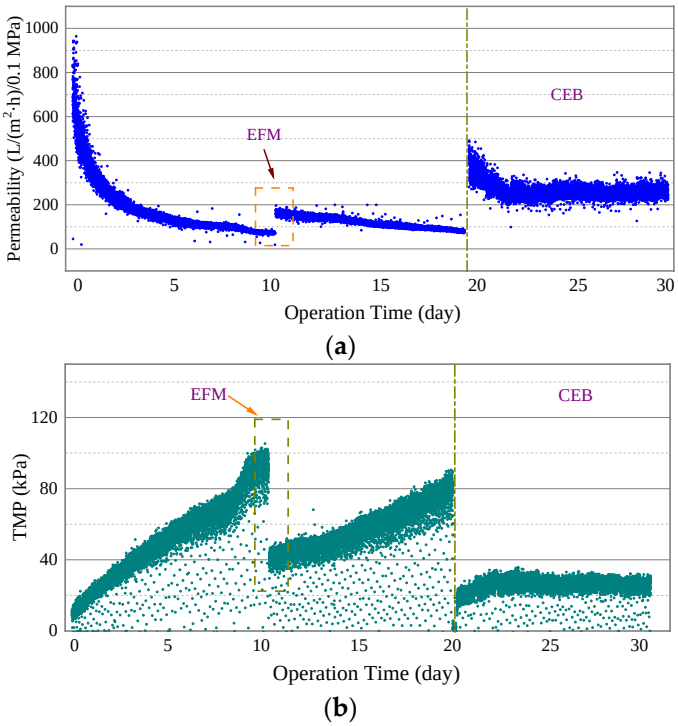


Figure 5. Variation trend of (**a**) permeability and (**b**) TMP under different cleaning methods.

3.3. Effect of SMT900-P80 Membrane Retention on Water Turbidity

In order to determine the water treatment performance of the SMT900-P80 module, the turbidity and retention ratio of the wastewater before and after treatment were analyzed. Figures 6 and 7 show the effects of different operating parameters on the turbidity and retention ratio, and it can be seen that the turbidity of the produced water was at a low level, the percentage of water with turbidity below 0.1 NTU was higher than 99.9%, and the percentage of water with turbidity below 0.05 NTU was higher than 99%. Operating parameters had little effect on the turbidity of the produced water. This was also confirmed by the changing trend of produced water turbidity in Figure 7b. The produced water turbidity fluctuated slightly in a very low range, and the trend difference was also caused by the raw water turbidity. The average turbidity of the influent water, as shown in Figure 6a, was 2.59 NTU, and the average retention ratio was 98.56%. The average turbidity of the influent water, shown in Figure 6b, was 3.56 NTU, and the average retention ratio was 99%. The average turbidity of the influent water, shown in Figure 7a, was 0.45 NTU, and the average retention ratio was 90.03%. These results indicate that the effect of membrane on turbidity was positively correlated with the influent turbidity, and the trend of retention ratio was consistent with the influent turbidity—the higher the influent turbidity, the higher the retention ratio of ultrafiltration membrane. According to the data in Figure 3, under the condition of high influent turbidity, the water permeability quickly dropped below 20 L/(m^2·h)/0.1 MPa, and TMP quickly rose to 40 kPa, while the data in Figure 5 under the condition of low turbidity show that the water permeability was maintained above 250 L/(m^2·h)/0.1 MPa, and TMP was kept near 30 kPa, indicating that, although the high influent turbidity does not affect water quality, it increases energy consumption and chemical reagent usage, resulting in lower membrane life.

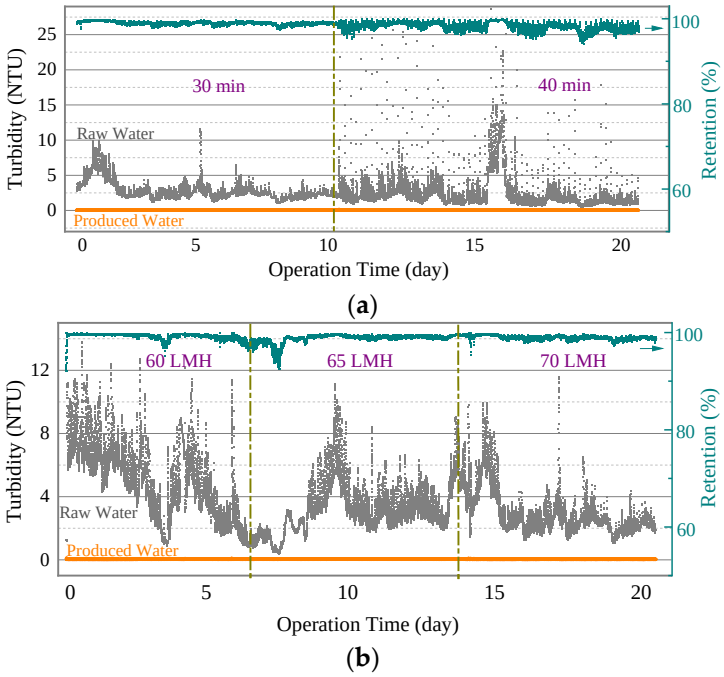


Figure 6. The influence of (**a**) filtration cycle and (**b**) operating flux on turbidity and retention ratio.

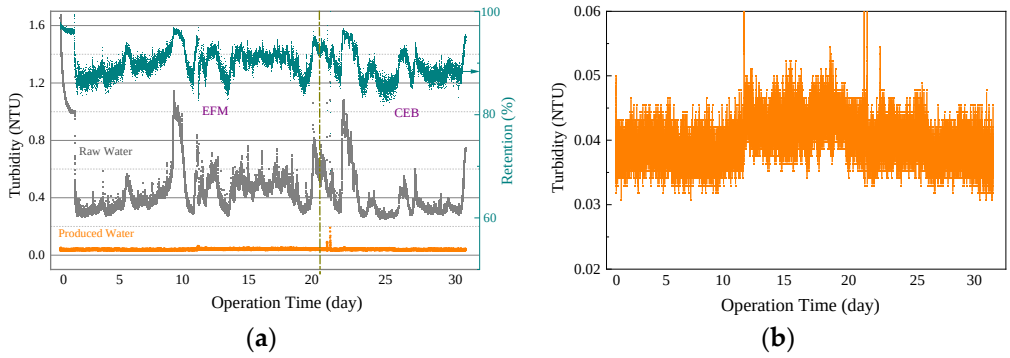


Figure 7. (**a**) The influence of cleaning methods on turbidity and retention ratio and (**b**) the enlarged part with a turbidity of 0.02–0.06 NTU in (**a**).

3.4. Membrane Fouling Ratio and Reversibility of SMT900-P80 Module

In order to analyze the effect of operation mode on fouling ratio during membrane filtration, the fouling ratios for different operating conditions of the SMT900-P80 module were investigated. Figure 8a shows the total fouling ratio, reversible fouling ratio, and irreversible fouling ratio calculated from the middle and last operation data during different filtration cycles. The difference between the total fouling ratio of 40 min and 30 min filtration cycle was not significant, but the irreversible fouling of 30 min filtration cycle was significantly lower than that of 40 min, especially in the early stage of operation. Figure 8b shows the fouling of the membrane at different operating fluxes; as can be observed, the increase in the volume of treated water led to an increase in the total fouling ratio and irreversible fouling ratio, and the total fouling ratio and irreversible fouling ratio of the high-flux (70 LMH) operation were significantly higher than the values of the low-flux (60 LMH and 65 LMH) operation. Figure 8c shows the fouling of the membrane before and after the EFM cleaning method and that at the end of the CEB operation method. The total fouling ratio and irreversible fouling ratio were significantly higher in the EFM cleaning method than in the CEB method, and the irreversible fouling ratio was greatly reduced in the CEB cleaning method, which was due to the accumulation and compaction of fouling, caused by long time chemical-free cleaning, which was avoided by the CEB method.

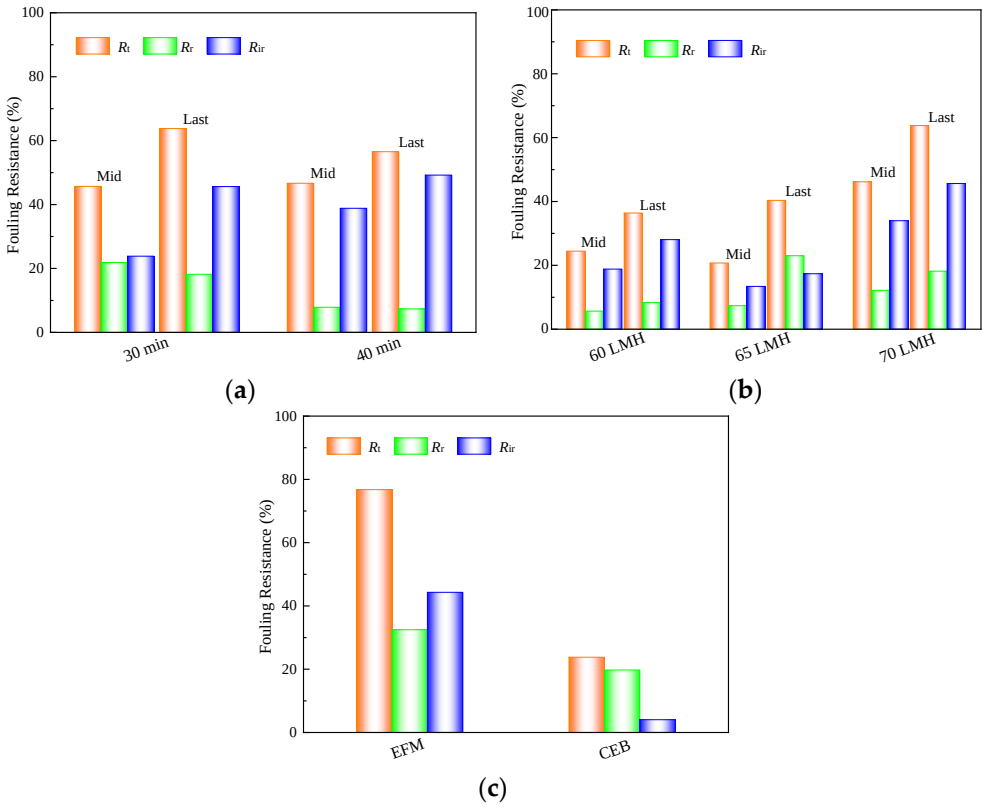


Figure 8. The influence of filtration cycle (**a**), operating flux (**b**), and cleaning method (**c**) on membrane fouling resistance of SMT900-P80 module.

3.5. Membrane Fouling Mechanism of SMT900-P80 Module

The microstructures of the fouled membrane inner surface, cross-section, and outer surface in Figure 9 show that, after fouling, some of the membrane pores on the membrane inner surface were blocked, the membrane cross-section still maintained porous structure, and the membrane outer surface was seriously fouled with a thick fouling layer. This indicates that the retained material was enriched on the outer surface of the membrane, and the inner surface of the membrane was basically not fouled, while the inner surface of the membrane was partially blocked due to the lack of flow and backwashing process, which increased fouling entering the inner surface of the membrane. The microstructure of the membrane after cleaning showed that the inner surface of the membrane had regained its porous structure, and the blockage of membrane pores had basically disappeared. Although no thick fouling layer could be observed on the outer surface of the membrane, there were still many pores that were blocked. This indicates that during operation, with the increase in treated water volume, the fouling accumulated on the outer surface of the membrane and formed a fouling layer, and TMP gradually increased and compacted the fouling layer, forming irreversible fouling.

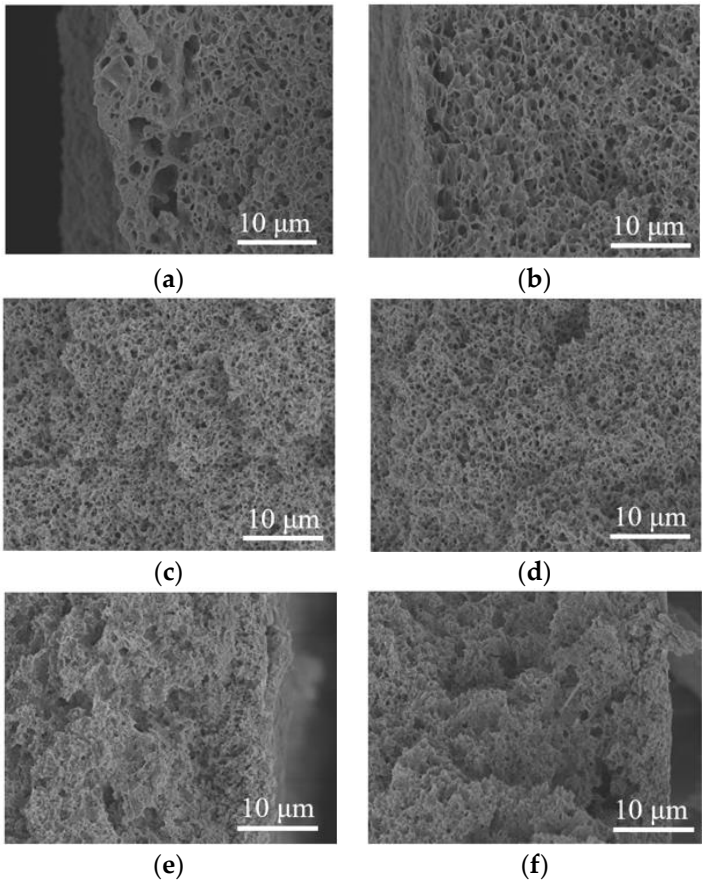


Figure 9. Microstructures of the (**a**,**b**) inner surface, (**c**,**d**) cross-section, and (**e**,**f**) outer surface of the fouled and cleaned membranes of SMT900-P80 module.

From the analysis results of element distribution on the outer surface of the membrane before and after cleaning in Table 3, it can be seen that the fouling elements were mainly O, Mn, and Fe, with the content reaching more than 10%, and a small amount of Na, Al, Si, Fe, S, P, and Ca. At the same time, the content ratio of C and F elements was much higher than those of the PVDF membrane. This result reveals that organic fouling and inorganic fouling existed at the same time, and the fouling degree was significant. After cleaning, only a small amount of O and Si remained, and the content ratios of C and F were close to those of the PVDF membrane, which indicates that the membrane had good reversibility of chemical cleaning. After cleaning, only a small amount of O and Si remained, and the ratios of C to F were greatly reduced, but they were still higher than those of the PVDF membrane, indicating that, although the inorganic fouling was basically removed, a small amount of organic fouling existed. The membrane had good reversibility of chemical cleaning.

Table 3. EDS analysis of fouled and cleaned membrane outer surface of SMT900-P80 module.

Fouled Membrane				Cleaned Membrane	
Element	**Mass/%**	**Element**	**Mass/%**	**Element**	**Mass/%**
S K	0.32	Pt M	5.43	Si K	0.03
Na K	0.43	F K	10.68	O K	3.09
Cu K	1.3	Mn K	13.09	Pt M	3.7
Si K	1.34	Fe K	15.82	C K	43.77
P K	1.97	C K	16.62	F K	49.41
Ca K	2.38	O K	26.59		
Al K	4.02				

4. Conclusions

The comparison results of the two membrane modules showed that, under similar effective membrane fiber lengths and same operation conditions, modules with lower packing density had more benefits for the whole system in terms of permeability and TMP; the SMT900-P80 module with lower packing density significantly reduced the average TMP, up to 60–70%, and increased permeability, up to 100%, which would indirectly lead to the difference in cleaning frequency and service life.

Meanwhile, the pilot test of SMT900-P80 PVDF hollow fiber ultrafiltration membrane module in the steel industry's wastewater treatment showed that the prolongation of filtration cycle and increase in operating flux during the operation would degrade the filtration performance of the membrane, and the percentage of irreversible fouling would increase significantly after long-term operation. Compared with EFM, CEB was a more effective cleaning method. It could maintain TMP (30 kPa) without any significant increase under the premise of ensuring the high-flux (65 LMH) operation of the membrane module, saving energy consumption, and presumably reducing the operating cost by further reducing the chemical reagents used in the cleaning process. After its operation, the proportion of water produced with turbidity below 0.05 NTU was more than 99%. The turbidity of the influent had a higher impact on the membrane retention ratio but little effect on the turbidity of the product, and the increase in influent turbidity led to a sharp increase in TMP, which increases the frequency of cleaning and chemical reagent usage. The results of this pilot test provide valuable points of reference for the industrial application of ultrafiltration membrane treatment of steel industry wastewater.

Author Contributions: Conceptualization, Y.Z.; data curation, Z.Y. and C.S.; investigation, H.B.; project administration, Y.Z. and L.H.; writing—original draft preparation, L.Z.; writing—review and editing, L.Z., H.B. and Y.Z. All authors have read and agreed to the published version of the manuscript.

Funding: This research was financially supported by the National Natural Science Foundation of China (No. 51974022), the Fundamental Research Funds for the Central Universities (Grant No. FRFMP-20-17), and the National Key Research and Development Program of China (Grant No. 2016YFC0401202).

Institutional Review Board Statement: Not applicable.

Informed Consent Statement: Not applicable.

Data Availability Statement: Data are contained within the article.

Conflicts of Interest: The authors declare no conflict of interest.

References

1. Long, H.; Lin, B.; Ou, Y.; Chen, Q. Spatio-temporal analysis of driving factors of water resources consumption in China. *Sci. Total Environ.* **2019**, *690*, 1321–1330. [CrossRef] [PubMed]
2. Yang, Y.; Yang, X.; Liang, L.; Gao, Y.; Cheng, H.; Li, X.; Zou, M.; Ma, R.; Yuan, Q.; Duan, X. Large-area graphene-nanomesh/carbon-nanotube hybrid membranes for ionic and molecular nanofiltration. *Science* **2019**, *364*, 1057–1062. [CrossRef] [PubMed]
3. Yeo, J.; Jung, G.S.; Martín-Martínez, F.J.; Beem, J.; Qin, Z.; Buehler, M.J. Multiscale Design of Graphyne-Based Materials for High-Performance Separation Membranes. *Adv. Mater.* **2019**, *31*, 1805665. [CrossRef] [PubMed]
4. Gui, Z.; Chen, X.; He, Y. Spatiotemporal analysis of water resources system vulnerability in the Lancang River Basin, China. *J. Hydrol.* **2021**, *601*, 126614. [CrossRef]
5. Choi, M.Y.; Theerthagiri, J.; Maia, G. 2D advanced materials and technologies for industrial wastewater treatment. *Chemosphere* **2021**, *284*, 131394. [CrossRef]
6. Devanesan, S.; AlSalhi, M.S. Effective removal of Cd^{2+}, Zn^{2+} by immobilizing the non-absorbent active catalyst by packed bed column reactor for industrial wastewater treatment. *Chemosphere* **2021**, *277*, 130230. [CrossRef]
7. Carrera, P.; Casero-Díaz, T.; Castro-Barros, C.M.; Méndez, R.; Val del Río, A.; Mosquera-Corral, A. Features of aerobic granular sludge formation treating fluctuating industrial saline wastewater at pilot scale. *J. Environ. Manag.* **2021**, *296*, 113135. [CrossRef]
8. Palani, G.; Arputhalatha, A.; Kannan, K.; Lakkaboyana, S.K.; Hanafiah, M.M.; Kumar, V.; Marella, R.K. Current Trends in the Application of Nanomaterials for the Removal of Pollutants from Industrial Wastewater Treatment—A Review. *Molecules* **2021**, *26*, 2799. [CrossRef]

9. Sun, W.; Xu, X.; Lv, Z.; Mao, H.; Wu, J. Environmental impact assessment of wastewater discharge with multi-pollutants from iron and steel industry. *J. Environ. Manag.* **2019**, *245*, 210–215. [CrossRef]
10. Li, A.L.; Wang, Z.H.; Sun, B.X.; Gao, S.W. Analysis of Water Consumption Intensity for Steel Production in China. *Mater. Sci. Forum* **2020**, *993*, 1465–1472. [CrossRef]
11. Tong, Y.; Zhang, Q.; Cai, J.; Gao, C.; Wang, L.; Li, P. Water consumption and wastewater discharge in China's steel industry. *Ironmak. Steelmak.* **2018**, *45*, 868–877. [CrossRef]
12. Jiao, K.; Yu, X.; Yuan, Z.; Zhang, Y.; Liu, J. Enhanced filtration performance of Al_2O_3-SiC porous ceramic composite tube depending on microstructure and surface property. *Desalin. Water Treat.* **2019**, *150*, 99–104. [CrossRef]
13. Biswas, P.; Bhunia, P.; Saha, P.; Sarkar, S.; Chandel, H.; De, S. In situ photodecyanation of steel industry wastewater in a pilot scale. *Environ. Sci. Pollut. Res. Int.* **2020**, *27*, 33226–33233. [CrossRef] [PubMed]
14. Colla, V.; Matino, I.; Branca, T.A.; Fornai, B.; Romaniello, L.; Rosito, F. Efficient Use of Water Resources in the Steel Industry. *Water* **2017**, *9*, 874. [CrossRef]
15. Zhang, K.; Zhao, Y.; Cao, H.; Wen, H. Multi-scale water network optimization considering simultaneous intra- and inter-plant integration in steel industry. *J. Clean. Prod.* **2018**, *176*, 663–675. [CrossRef]
16. Wu, L.; Liu, Y.; Hu, J.; Feng, X.; Ma, C.; Wen, C. Preparation of polyvinylidene fluoride composite ultrafiltration membrane for micro-polluted surface water treatment. *Chemosphere* **2021**, *284*, 131294. [CrossRef]
17. Santosh, V.; Palodkar, K.K.; Veerababu, P.; Sainath, A.V.S.; Reddy, A.V.R. Polysulfone with glycopolymer for development of antifouling ultrafiltration membranes. *J. Polym. Res.* **2021**, *28*, 240. [CrossRef]
18. Güneş-Durak, S. Examination and Evaluation of a Metal Industry Wastewater Treatment and Recycle. *Eurasian J. Environ. Res.* **2018**, *1*, 8–17.
19. Ashok Kumar, S.; Subathra, K.; Srinivasan, G.; Sundaramurthy, J.; Gnanasekaran, G.; Kanimozhi, G.; Govindaradjane, S. Impact of Tween-80 and Deep Eutectic Solvent-Based Micellar-Enhanced Ultrafiltration in Dairy Wastewater Treatment. *Chem. Eng. Technol.* **2021**, *44*, 913–922. [CrossRef]
20. Sponza, D.T. Treatment of Textile Industry Wastewater by Sequential Hybrid Processes Photo-Fenton, Ultrafiltration (UF), Reverse Osmosis (RO) and Recovery of some Dyes, Salt and Perfluoroalkyl Sulfonate from the Retentate. *J. Membr. Sci. Technol.* **2020**, *10*, 214.
21. Öztel, M.D.; Kuleyin, A.; Akbal, F. Treatment of zinc plating wastewater by combination of electrocoagulation and ultrafiltration process. *Water Sci. Technol.* **2020**, *82*, 663–672. [CrossRef] [PubMed]
22. Benito, A.; Garcia, G.; Gonzalez-Olmos, R. Fouling reduction by UV-based pretreatment in hollow fiber ultrafiltration membranes for urban wastewater reuse. *J. Membr. Sci.* **2017**, *536*, 141–147. [CrossRef]
23. Yoon, S.-H.; Kim, H.-S.; Yeom, I.-T. Optimization model of submerged hollow fiber membrane modules. *J. Membr. Sci.* **2004**, *234*, 147–156. [CrossRef]
24. Ye, Y.; Sim, L.N.; Herulah, B.; Chen, V.; Fane, A.G. Effects of operating conditions on submerged hollow fibre membrane systems used as pre-treatment for seawater reverse osmosis. *J. Membr. Sci.* **2010**, *365*, 78–88. [CrossRef]
25. Wang, Q.; Peng, Y.; Ji, X.; Hadi, M.K.; Zhang, S.; Tang, J.; Ran, F. Conductive 3D networks in a 2D layer for high performance ultrafiltration membrane with high flux-retention and robust cyclic stability. *J. Membr. Sci.* **2021**, *640*, 119781. [CrossRef]
26. Bai, H.; Lin, Y.; Qu, H.; Zhang, J.; Zheng, X.; Tang, Y. Technical and Economic Evaluation of WWTP Renovation Based on Applying Ultrafiltration Membrane. *Membranes* **2020**, *10*, 180. [CrossRef]